ELSEVIER

Biochimica et Biophysica Acta 1412 (1999) 118–128

BIOCHIMICA ET BIOPHYSICA ACTA
BBA

www.elsevier.com/locate/bba

Kinetic modeling of rotary CF_0F_1-ATP synthase: storage of elastic energy during energy transduction

Oliver Pänke [1], Bernd Rumberg *

Max-Volmer-Institut, Technische Universität Berlin, D-10623 Berlin, Germany

Received 7 April 1999; accepted 3 May 1999

Abstract

F_0F_1-ATP synthase uses proton-motive force to produce ATP from ADP and P_i. With regard to its rotary mechanics, this energy transducing molecular machine assumes a unique position among all enzymes. In the work presented here we put forward a detailed functional model which is based on experimental results obtained with ATP synthase from spinach chloroplasts. We focus on the role of the elastic element, realized by the stalk-like subunit γ, whose function is energy transduction between F_0 and F_1 taking into account the H^+/ATP coupling ratio of four. Fitting parameters are the rate constants and the torsional rigidity of γ, which have been adjusted according to the experimental results where the influence of transmembrane ΔpH on the rates of ATP synthesis/hydrolysis is put to the test. We show that the input and output of torsional energy are regulated by purely statistical principles, giving rise to the amount of transiently stored energy to be sliding, depending on ΔpH. During conditions of maximal turnover γ turns out to be wound up towards 102° which corresponds to a torque of $5.3 \cdot 10^{-20}$ N·m.

Keywords: F_0F_1-ATP synthase; Proton transport; Energy transduction; Enzyme kinetics; Motor protein

1. Introduction

F_0F_1-ATP synthase, which is found intrinsic to the membranes of bacteria, chloroplasts and mitochondria, uses proton-motive force to produce ATP from ADP and inorganic phosphate (for a recent review see [1]). The H^+/ATP coupling ratio is four [2–4]. This at least has been shown for ATP synthases from chloroplasts and cyanobacteria and should be the same for synthases from other sources supposing a c/(αβ) subunit ratio of four [5]. The crucial point of interest is the mechanism of energy transduction between the membrane embedded F_0 portion, where the energy releasing proton transport takes place, and the extrinsic F_1 portion, where the energy consuming ATP synthesis occurs. The hypothesis of a rotary mechanism has been published already 18 years ago and has since been elaborated further by work of Boyer and his group [6,7]. According to this proposal the γ subunit sticks through the center of the hexagonal structure of the $(\alpha\beta)_3$ ensemble of F_1 and H^+-driven rotation of γ relative to $(\alpha\beta)_3$ induces the binding change in F_1 in which three binding sites are alternately involved in nucleotide binding, conversion and release. First direct evidence for this hypothetical concept came from work of Walker et al.

* Corresponding author. Fax: +49 (30) 31421122; E-mail: rumberg@echo.chem.tu-berlin.de

[1] Present address: AG Biophysik, Universität Osnabrück, D-49069 Osnabrück, Germany.

0005-2728/99/$ – see front matter
PII: S0005-2728(99)00059-6

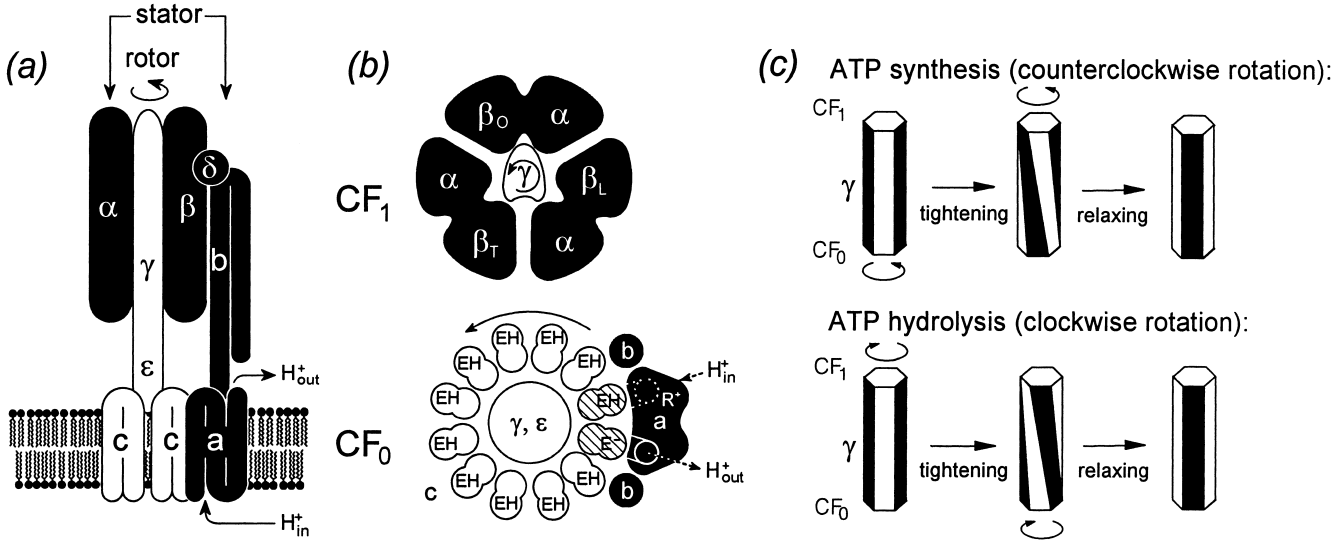

Fig. 1. Basic structural model of rotary CF_0F_1-ATP synthase. (a) Complete ensemble of subunits according to [17]. Stator elements are displayed in black and rotor elements in white. (b) Cross-sections of CF_0 and CF_1 seen from above. Anticlockwise rotation corresponds to ATP synthesis according to [12]. E^- and R^+ denote the charged species of amino acids Glu^{61} and Arg^{211} which are important during torque generation in CF_0 [18,19]. Symbols O, L, T refer to the conformational states open, loose, tight according to [7]. (c) Visualization of the sequence of torsional states of the elastic element γ during ATP synthesis/hydrolysis.

on the crystal structure of bovine heart F_1 [8]. Their results confirmed the assumptions of γ to form an axis relative to $(\alpha\beta)_3$ and of $(\alpha\beta)_3$ to bear three substrate binding sites which are equivalent in the time average but each moment differently occupied by ADP, ATP or empty. Using site-directed tryptophan fluorescence, Senior et al. showed that all three binding sites must be filled to bring about maximal enzyme turnover [9]. By application of different techniques, convincing evidence has now been accumulated that indeed rotation of the γ subunit relative to the $(\alpha\beta)_3$ ensemble is involved during energy transduction [10–13]. Moreover, it has been demonstrated that one revolution takes place in three discrete steps [14–16]. Hypothetical models for torque generation by F_0 have been presented by several authors [17–19]. Recently, Junge et al. outlined the structural basis of a rotary mechanism of energy transduction in F_0F_1-ATP synthase in detail, taking into account all knowledge so far available [17,20]. According to this picture the rotor is composed of the subunit complex $\gamma\varepsilon c_{12}$, while the stator is made up of the ensemble $(\alpha\beta)_3\delta b_2 a$ (see Fig. 1a,b).

In a previous paper we introduced the kinetic modeling of the F_0F_1-ATP synthase where we considered already the rotary character of this enzyme, although then on a merely hypothetical basis [21]. We introduced γ as an elastic element which accumulates rotational energy generated by F_0 before it is transferred to F_1 (see Fig. 1c). In the present article we kinetically modeled an elastically coupled, rotary mechanism of F_0F_1-ATP synthase based on experimental results obtained with ATP synthase from spinach chloroplasts. Preliminary results have been presented elsewhere [22].

2. Materials and methods

Experiments were performed with suspensions of spinach thylakoids under conditions of thiol-modulated and activated ATP synthases as described in a previous paper [21]. We used fixed values of pH_{out} 8.00, pMg 2.52, temperature 20°C and ionic strength 0.07 M. The thylakoid lumen was acidified by continuous illumination. The intravesicular pH was measured as described in [4]. The simulation was carried out by numerical routines on a standard PC. The set of five linear algebraic equations was solved with regard to the unknown concentrations of enzyme species by application of Crout's algorithm of LU decomposition.

3. Functional model of F_0F_1-ATP synthase

3.1. General concept

The complete reaction scheme used here is presented in Fig. 2. It is essentially the same as previously given [21]. The following details are taken into account:

1. At any time, all three αβ pairs display different conformational states, representing an open (O), a loosely closed (L), and a tightly closed (T) binding site.
2. Substrate exchange with the medium is practically restricted to the O site with competitive binding between ATP and ADP or P_i and random binding (or release) of ADP and P_i.
3. Counterclockwise 120° rotation (viewed from top) of γ within the ring of $(\alpha\beta)_3$ drives the concerted binding change O→L, L→T, T→O.
4. Conversion of ADP+P_i into ATP+H_2O is coupled with the L→T transition.
5. F_0 operates as an H^+-driven stepper motor with anticlockwise rotation of the c_{12} ring relative to subunit a. The ring moves by one position or 30° on for each H^+ which is translocated down the gradient from inside to outside (see also Fig. 1b).
6. Subunit γ acts as an elastic element like a cylindrical torsional bar, which is wound up at the bottom by the F_0 motor in a series of 30° rotational steps and which relaxes at the top by 120° rotational steps coupled with the binding change in F_1 (see also Fig. 1c). The torsional states of γ, which differ by 30° angular distance between bottom and top, are indicated as A_j ($j=0, \pm1, \pm2, \ldots$).
7. The principle of microreversibility is imposed on every single reaction step, which means that during ATP hydrolysis γ is wound up at the top in

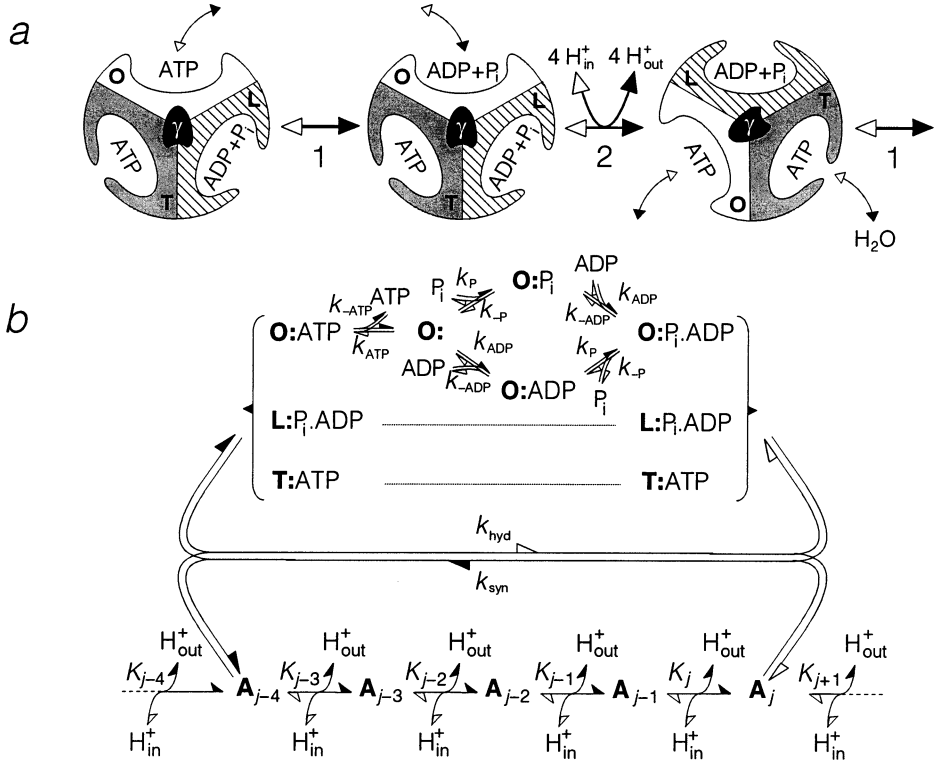

Fig. 2. (a) Schematic presentation of the binding change mechanism for ATP synthesis/hydrolysis as described in the text. Sections denoted O, L, T refer to $\alpha\beta_O$, $\alpha\beta_L$, $\alpha\beta_T$ in Fig. 1b. Solid arrows refer to synthesis of ATP and open arrows to hydrolysis. The entire catalytic cycle is complete in 3-fold repetition of reaction steps 1 and 2. (b) Detailed reaction pattern according to (a). Symbols A_j refer to the torsional states of subunit γ.

clockwise direction and relaxation takes place at the bottom, where it is coupled with H^+ pumping from outside to inside (see Fig. 1c).

The Gibbs energy which is stored primarily in the transmembrane H^+ gradient and which is available during H^+ transport from inside to outside is described by the electrochemical potential difference for H^+ according to:

$$\Delta\tilde{\mu}_{H^+} = -2.3RT\cdot\Delta pH + F\cdot\Delta\Psi \quad (1)$$

where $\Delta pH = pH_{out} - pH_{in}$ denotes the outside-minus-inside pH difference and $\Delta\Psi$ the corresponding electrical potential difference. The A states store torsional energy at the expense of $\Delta\tilde{\mu}_{H^+}$ (see Fig. 2b). Transitions between two subsequent A states occur according to:

$$A_{j-1} \underset{k_j^-}{\overset{k_j^+}{\rightleftharpoons}} A_j \ (j = 0, \pm1, \pm2 \ldots) \quad (2)$$

Theoretical considerations show that the rate constants k_j^+, k_j^- should be subject to the separate influence of pH_{in}, pH_{out} and $\Delta\Psi$ (B. Rumberg et al., in preparation). This means that with respect to the individual rate constants ΔpH and $\Delta\Psi$ are not equivalent according to Eq. 1. Experimentally, this expectation is confirmed by kinetic studies during the induction phase of the activation process, obtained with reconstituted ATP synthases from chromatophores of *Rhodobacter capsulatus* subject to ΔpH and $\Delta\Psi$ jumps [23]. Exchangeability between ΔpH and $\Delta\Psi$ according to Eq. 1 is restricted to the equilibrium of Eq. 2, namely:

$$K_j = \frac{A_j}{A_{j-1}} = \exp[-(\Delta\tilde{\mu}_{H+} + \Delta W_j)/RT] \quad (3)$$

where the symbols A_j denote species concentration, K_j the equilibrium constant, and ΔW_j the torsional energy difference. Experimental results of steady-state rates of ATP synthesis obtained with reconstituted ATP synthases from both spinach chloroplasts [24] and chromatophores from *R. capsulatus* [23] show that ΔpH and $\Delta\Psi$ in this case are in fact exchangeable according to Eq. 1. This means that the transitions between subsequent A states are obviously not of rate-limiting character with regard to the overall reaction sequence of the ATP synthase. Thus, within the framework of steady-state conditions, these transitions may be described by fast equilibria assumptions according to Eq. 3. By this procedure the mathematical modeling of the reaction system is simplified considerably. In this case the five species of O states are calculable from a system of four linear independent steady-state equations and one balance equation. On the basis of the reaction sequence $O{:}ATP \rightarrow O{:} \rightarrow O{:}ADP$ (alternatively $O{:}P) \rightarrow O{:}P.ADP \rightarrow O{:}ATP$ (see Fig. 2b), this set of equations may be formulated as follows (where x denotes the fraction number of the indicated species and ADP, P_i, ATP denote the corresponding molar concentrations):

$$k_{syn}\cdot x_{O:P.ADP} + k_{ATP}\cdot ATP\cdot x_{O:} - (k_{hyd} + k_{-ATP})\cdot x_{O:ATP} = 0 \quad (4a)$$

$$k_{-ATP}\cdot x_{O:ATP} + k_{-P}\cdot x_{O:P} + k_{-ADP}\cdot x_{O:ADP} - (k_{ATP}\cdot ATP + k_P\cdot P_i + k_{ADP}\cdot ADP)\cdot x_{O:} = 0 \quad (4b)$$

$$k_{ADP}\cdot ADP\cdot x_{O:} + k_{-P}\cdot x_{O:P.ADP} - (k_{-ADP} + k_P\cdot P_i)\cdot x_{O:ADP} = 0 \quad (4c)$$

$$k_{ADP}\cdot ADP\cdot x_{O:P} + k_P\cdot P_i\cdot x_{O:ADP} + k_{hyd}\cdot x_{O:ATP} - (k_{-ADP} + k_{-P} + k_{syn})\cdot x_{O:P.ADP} = 0 \quad (4d)$$

$$x_{O:ATP} + x_{O:} + x_{O:P} + x_{O:ADP} + x_{O:P.ADP} = 1 \quad (4e)$$

The overall reaction rate may be calculated from:

$$v = k_{syn}\cdot x_{O:P.ADP} - k_{hyd}\cdot x_{O:ATP} \quad (5)$$

The rate constants k_{syn}, k_{hyd} refer to the binding change reactions and depend on the probability that torsional energy is available from γ.

3.2. Probability distribution of torsional energy accumulation in γ

The torque needed for the winding up of γ depends on the torsional angle φ (in radian units) as follows:

$$M = M^*\cdot\varphi = M^*\cdot\frac{2\pi}{12}\cdot j \quad (6)$$

where M^* is the torsional rigidity of γ and j is the number of elementary rotary steps. The correspond-

ing elastic energy per mol of γ is:

$$W_j = N_A \cdot \int_0^j M \cdot d\varphi = \alpha \cdot j^2 \text{ where } \alpha = \frac{1}{2} N_A \cdot M^* \cdot \left(\frac{2\pi}{12}\right)^2 \quad (7)$$

and N_A = Avogadro number. The energy change per elementary step increases with increasing j and comes to:

$$\Delta W_j = W_j - W_{j-1} = \alpha \cdot (2j-1) \quad (8)$$

Using Eqs. 3 and 8 the probability p_j of a definite torsional state A_j is calculated as follows (for derivation see Appendix A.1):

$$p_j = \frac{A_j}{\sum_{j=-\infty}^{+\infty} A_j} = \frac{\exp[-(\Delta\tilde{\mu}_{H^+} \cdot j + \alpha \cdot j^2)/RT]}{\sum_{j=-\infty}^{+\infty} \exp[-(\Delta\tilde{\mu}_{H^+} \cdot j + \alpha \cdot j^2)/RT]} \quad (9)$$

Graphs of p_j in dependence on the torsional number j according to Eq. 9 are shown in Fig. 3a. The resulting bell-shaped Gaussian curves are shifted to higher states with increasing $\Delta\tilde{\mu}_{H^+}$. Peak position and half-width are calculable from (for derivation see Appendix A.2):

$$j_{peak} = -\Delta\tilde{\mu}_{H^+}/2\alpha \text{ and } \Delta j_{1/2} = 2\sqrt{(\ln 2) \cdot RT/\alpha} \quad (10a, b)$$

The average winding up of γ and the corresponding torque in dependence on the protonic electrochemical potential difference are calculable from:

$$\langle j \rangle = \sum_{j=-\infty}^{+\infty} (j \cdot p_j) \equiv j_{peak} \quad (11a)$$

$$\langle M \rangle = M^* \cdot \frac{2\pi}{12} \cdot \langle j \rangle \equiv -\frac{\Delta\tilde{\mu}_{H^+}}{2\pi/12} \quad (11b)$$

Results are shown in Fig. 4.

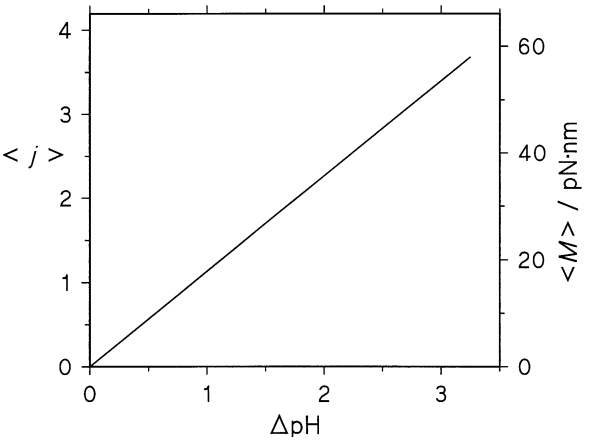

Fig. 4. Calculated influence of ΔpH at conditions of $\Delta\Psi = 0$ on the mean values of the torsional state number j according to Eq. 11a and the corresponding torque M acting on γ according to Eq. 11b ($M^* = 3.0 \cdot 10^{-20}$ N·m, $T = 293$ K).

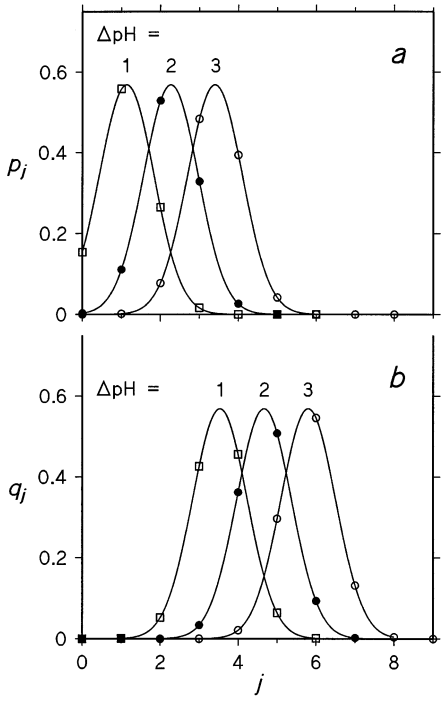

Fig. 3. Calculated influence of the torsional state number j on (a) the state probability p_j according to Eq. 9 and (b) the reaction probability q_j according to Eq. 16 for different values of ΔpH at conditions of $\Delta\Psi = 0$ ($M^* = 3.0 \cdot 10^{-20}$ N·m, $\kappa = 0.6$, $T = 293$ K). See text for further explanations.

3.3. Calculation of the binding change rate constants

The binding change for ATP synthesis is coupled with the torsional relaxation of γ from state j to state $j-4$. The corresponding rate constants k_{syn}, k_{hyd} are obtained by application of the transition-state theory:

$$k_{syn} = k_{syn}^{\circ} \cdot \sum_{j=-\infty}^{+\infty} [p_j \cdot \exp(-\Delta W^*_{syn}/RT)] \quad (12a)$$

$$k_{hyd} = k_{hyd}^{\circ} \cdot \sum_{j=-\infty}^{+\infty} [p_{j-4} \cdot \exp(-\Delta W^*_{hyd}/RT)] \quad (12b)$$

where ΔW^*_{syn}, ΔW^*_{hyd} are the changes of the transition-state energy caused by the torque of γ. The position of the transition state along the angular path of γ is:

$$j^* = j - 4\kappa \quad (13)$$

where κ is a number between 0 and 1. Taking into account (with recourse to Eqs. 7 and 13)

$$\Delta W^*_{syn} = W_{j^*} - W_j = -8\alpha \cdot \kappa \cdot (j - 2\kappa) \quad (14a)$$

$$\Delta W^*_{hyd} = W_{j^*} - W_{j-4} = 8\alpha \cdot (1-\kappa) \cdot [j - 2(1+\kappa)] \quad (14b)$$

we obtain finally after some rearrangements:

$$k_{syn} = k_{syn}^{\circ} \cdot D \quad (15a)$$

$$k_{hyd} = k_{hyd}^{\circ} \cdot D \cdot \exp(4\Delta\tilde{\mu}_{H^+}/RT) \quad (15b)$$

where

$$D = \sum_{j=-\infty}^{+\infty} [p_j \cdot \exp[8\alpha \cdot \kappa \cdot (j - 2\kappa)/RT]]$$

By application of Eqs. 12a and 14a the reaction probability q_j for each single A_j state is calculable as follows:

$$q_j = \frac{p_j \cdot \exp(-\Delta W^*_{syn}/RT)}{\sum_{j=-\infty}^{+\infty} [p_j \cdot \exp(-\Delta W^*_{syn}/RT)]}$$

$$= \frac{p_j \cdot \exp(8\alpha \cdot \kappa \cdot (j - 2\kappa)/RT)}{\sum_{j=-\infty}^{+\infty} [p_j \cdot \exp(8\alpha \cdot \kappa \cdot (j - 2\kappa)/RT)]} \quad (16)$$

Results are shown in Fig. 3b. The bell-shaped curves are identical to those describing p_j but are shifted by 4κ positions to higher j values (for derivation see Appendix A.3). The reason for this shift is the increasing backpressure of the elastic element which initially overcompensates the decreasing state probability.

4. Simulation of the experimental data

During steady-state conditions and with an ionic strength of 70 mM the proton-motive force across the thylakoid membrane consists of a pH difference only, without contribution of an electrical potential difference ($\Delta\Psi = 0$) [25,26]. In this case the protonic electrochemical potential difference simplifies from Eq. 1 to:

$$\Delta\tilde{\mu}_{H^+} = -2.3RT \cdot \Delta pH = -2.3RT \cdot \lg[(H^+)_{in}/(H^+)_{out}] \quad (17)$$

where curved brackets denote proton activity. Under such conditions, we measured the rates of ATP synthesis/hydrolysis in dependence on the concentrations of ADP, P_i, ATP and the activity of H^+_{in} for a fixed

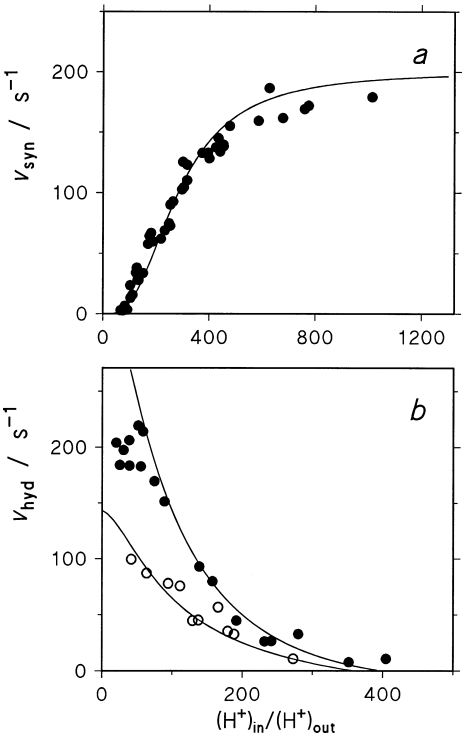

Fig. 5. Influence of the activity ratio $(H^+)_{in}/(H^+)_{out}$ (with $(H^+)_{out}$ fixed to 10 nM) on (a) the rate of ATP synthesis v_{syn} (molecules ATP produced per single enzyme and second) and (b) the rate of ATP hydrolysis v_{hyd} (molecules ATP hydrolyzed per single enzyme and second). Reaction conditions were (a) 1 mM ADP, 1 mM P_i, 10 μM ATP, (b) 3 mM ATP, 50 μM ADP, 1 mM P_i (solid circles) or 200 μM ATP, 50 μM ADP, 100 μM P_i (open circles). Inserted curves have been calculated according to the simulation procedure presented in the text.

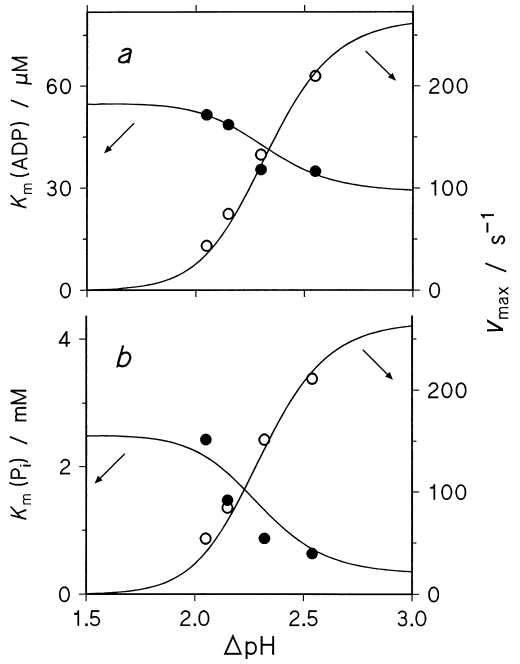

Fig. 6. Influence of ΔpH (with pH_{out} fixed to 8.00) on he maximal rate of ATP synthesis v_{max} (open circles) and the Michaelis constant K_m (solid circles) with respect to (a) variable ADP in the presence of 10 mM P_i and (b) variable P_i in the presence of 1 mM ADP. The inserted curves have been calculated according to the simulation procedure presented in the text.

activity of H^+_{out}. The above outlined model allows simulation of all these data. Fitting parameters are the various rate constants and, in addition, M^* and κ. The rate constants of substrate association/dissociation are taken over from [21]. $k_{syn}°$, M^* and κ have been adjusted for optimal fit to the experimental results in Fig. 5, where the influence of $(H^+)_{in}$ on ATP synthesis/hydrolysis is put to the test. $k_{hyd}°$ is calculable from $k_{syn}°$ and the overall equilibrium constant of ATP synthesis, $K_\Sigma = 2.4 \cdot 10^{-6}$ M^{-1} (equivalent to $\Delta_r G_P° = 31.5$ kJ mol^{-1} [4]), according to:

$$k_{hyd}{}^{\circ} = \frac{1}{K_\Sigma} \cdot \frac{k_{syn}{}^{\circ} \cdot k_{ADP} \cdot k_P \cdot k_{-ATP}}{k_{-ADP} \cdot k_{-P} \cdot k_{ATP}} \quad (18)$$

All constants are listed in Table 1. The simulation of the experimental data turns out to be quite sufficient.

For ATP synthesis hyperbolic Michaelis-Menten kinetics with respect to both ADP and P_i are observed (data not shown, see [21]). Most interestingly, in both cases the Michaelis constant K_m is decreased along with the maximal velocity increase caused by the enlargement of the transmembrane ΔpH. The simulated results are in full accord with these experimental findings (see Fig. 6). The kinetic modeling shows that with increasing ΔpH the binding change in synthesis direction is accelerated and the release of ATP becomes rate-limiting. This effect lowers the K_m values of ADP and P_i [21].

5. Discussion

5.1. General comment

With respect to its rotary mechanics of energy transduction the F_0F_1-ATP synthase assumes a unique position among all enzymes (albeit vacuolar ATPases likewise have a rotary mechanism [27] and probably some enzymes handling DNA such as T7 helicase [28] and Rho [29]). In the work presented here, we focus on the role of the elastic element (presumably realized by subunit γ) whose function is energy transmission between F_0 and F_1. We show that input and output of elastic energy is regulated by

Table 1
Model parameter values used for simulation of the experimental data

(a) Rate constants of substrate association/dissociation (from [21])		
$k_{ATP} = 2.08 \cdot 10^6$ M^{-1} s^{-1}	$k_{-ATP} = 2.70 \cdot 10^2$ s^{-1}	($K_d = 130$ µM)
$k_{ADP} = 8.90 \cdot 10^6$ M^{-1} s^{-1}	$k_{-ADP} = 4.90 \cdot 10^2$ s^{-1}	($K_d = 55$ µM)
$k_P = 8.10 \cdot 10^5$ M^{-1} s^{-1}	$k_{-P} = 2.03 \cdot 10^3$ s^{-1}	($K_d = 2.5$ mM)
(b) Further constants (from this work)		
Specific binding change rate constants		$k_{syn}° = 1.15 \cdot 10^{-3}$ s^{-1}
		$k_{hyd}° = 4.50 \cdot 10^5$ s^{-1}
Torsional rigidity of γ (elastic element)		$M^* = 3.0 \cdot 10^{-20}$ N.m
Position of the binding change transition state κ		κ = 0.6

purely statistical principles, which means that the amount of transiently stored elastic energy is sliding, depending on the protonic electrochemical potential difference $\Delta\tilde{\mu}_{H^+}$ or, in the case of $\Delta\Psi = 0$, exclusively on the transmembrane pH difference ΔpH (see Figs. 3 and 4). During the conditions of maximal ATP synthesis turnover ($\Delta\Psi = 0$, $\Delta pH = 3$) the elastic element γ is wound up towards $j_{peak} = 3.4$ (torsional angle of 102°) at an average which corresponds to a torque $M = 5.3 \cdot 10^{-20}$ N·m (data from Fig. 4). The binding change gives rise to the oscillation of j values between $j_{peak} + 4\kappa = 5.8$ and $j_{peak} + 4\kappa - 4 = 1.8$. At the same time the rotational rate comes to $v_{rot} = v_{syn}/3 = 64\ s^{-1}$ (see Fig. 5a). The energy output per revolution invariably amounts to $E/3 = \Delta_r G_P = \Delta_r G_P^\circ + RT \cdot \ln(ATP/(ADP \cdot P_i)) = 37.1$ kJ mol^{-1} (taking into account the experimental conditions of Fig. 5a). However, the power increases along the ΔpH scale from $P = 0$ at the beginning to $P = E \cdot v_{rot} = 7.13 \cdot 10^3$ kW at $\Delta pH = 3$. The efficiency drops continuously, starting from $\eta = 1$ and passing $\eta = E/(12\ \Delta\tilde{\mu}_{H^+}) = 0.55$ at $\Delta pH = 3$.

5.2. Torsional rigidity of γ

By optional fit of the kinetic data we determined the torsional rigidity of the elastic element as $M^* = 3.0 \cdot 10^{-20}$ N·m. Direct information on the elastic properties of subunit γ is not available. However, a rough estimate is possible on the basis of data from the literature for single actin filaments which are likewise modeled by an α-helical coiled-coil structure. The torsional rigidity related to unit filament length has been directly determined as $M^*_{actin} \cdot l_{actin} = 8 \cdot 10^{-26}$ N·m^2 [30]. This value may be adjusted to the properties of γ if the different size parameters are taken into account according to $M^* = (M^*_{actin} \cdot l_{actin}/l_\gamma) \cdot (r_\gamma/r_{actin})^4$, assuming both actin and γ to be homogeneous cylinders of length l and radius r [31]. X-Ray structure analysis indicates $r_{actin} = 2.8$ nm [30] and is compatible with $l_\gamma = 5$ nm (region of γ capable of torsion), $r_\gamma = 0.6$ nm [8]. On the basis of these values we calculate $M^* = 3.4 \cdot 10^{-20}$ N·m, which is close to the value obtained by optimal fit of kinetic data in this study. This estimation neglects possible elastic contributions from the stator due to elastic distortions of subunits b and even β.

5.3. Separate influence of pH_{out} and $\Delta\Psi$

Our simulation procedure is based on the assumption of fast H^+-coupled transitions between adjacent A_j states. As a consequence, the simulated kinetics of ATP synthesis/hydrolysis turn out to be dependent on the value of $\Delta\tilde{\mu}_{H^+}$ only, independent of the choice of ΔpH and $\Delta\Psi$ to yield a definite $\Delta\tilde{\mu}_{H^+}$. This behavior is in accordance with experimental results reported in the literature [23,24]. Moreover, the simulated kinetics turn out to be independent of the preselected pH_{out} value. This is also in accordance with the data in the literature, at least in the region $pH_{out} = 7.5$–8.5 [32]. However, this picture changes above $pH_{out} = 8.5$. In this region, a progressive slowdown of ATP synthesis is observed when data belonging to different pH_{out} values are compared on the basis of a common ΔpH scale [32]. This behavior indicates that the H^+-driven winding-up transitions of succeeding A_j states become rate-limiting because of their slowdown due to the decreased H^+ activity on the inner side of the membrane. A corresponding behavior may be predicted for the region below $pH_{out} = 7.5$ where the H^+ release on the outer side of the membrane is slowed down due to the increased H^+ activity. These results prove the simulation procedure presented here to be an approximation within the limit of $pH_{out} = 7.5$–8.5. Consequently, outside this region also a separate influence of the electrical potential difference $\Delta\Psi$ should be observed. Relevant experimental data are not available as yet. Recently, Kaim and Dimroth [33] presented evidence that in the case of *Escherichia coli* ATP synthase ΔpH and $\Delta\Psi$ are generally unequivalent driving forces for ATP synthesis, irrespective of the preselected pH_{out} value. In experiments with *E. coli* ATP synthases reconstituted into proteoliposomes they showed that $\Delta\Psi$ is a mandatory force for ATP synthesis. Within the framework of the modeling concept presented here this result may be interpreted as follows: in the case of *E. coli* ATP synthase the assumption that the H^+-coupled transitions between adjacent A_j states are fast has to be canceled. A substantial slowdown of the H^+-driven winding-up transitions of succeeding A_j states may be caused by a higher value of the torsional rigidity of the elastic element. Theoretical treatments show that this effect is preferentially compensated by an increased $\Delta\Psi$ as compared

to an increase in ΔpH. An extended modeling taking these considerations into account will be presented elsewhere (B. Rumberg et al., in preparation).

5.4. Details of the binding change concept

With regard to the binding change concept used here (see Fig. 2) we would like to clear up four special points. (1) Our model is based on the assumption of three catalytically active binding sites, one on each αβ subunit pair. This is a logical prerequisite for a rotary mechanism [6,7]. Experimental evidence has been put forward by structural arguments [8]. (2) The binding sites differ with respect to their substrate binding affinity being low/medium/high for states O/L/T. With respect to CF_0F_1, literature values of the corresponding K_d values for ADP/ATP are 55/130 μM for state O (from this work, see Table 1), 1/3 μM for state L (from inhibition of proton slip, see [34]) and 700/15 nM for state T (from unisite catalysis, see [35,36]. With respect to ATP, lower K_d values of 200 pM for EF_1 [37] and 1 pM for MF_1 [38] have been reported). The association constant k_+ in each case is diffusion controlled and amounts to approx. 10^6 ... 10^7 M^{-1} s^{-1} (see Table 1 and unisite data from [39,40]). The dissociation constant k_- is calculated according to $k_- = k_+ \cdot K_d$. The k_- values come to very roughly 200/5/0.02 (ATP) ... 5 (ADP) s^{-1} for states O/L/T. Our binding change concept assumes nucleotide release from site O to be the overall rate-limiting reaction step during rapid enzyme turnover. This has been demonstrated for ATP synthesis (release of ATP) as well as ATP hydrolysis (release of ADP) [21]. (3) Our concept restricts substrate exchange to the O state. This supposition accounts for the experimental fact of competitive binding between ATP and ADP or P_i. This has been shown unequivocally, again for conditions of both ATP synthesis and hydrolysis [21,41]. We do not exclude substrate exchange at the level of states L and even T in general. However, as far as rapid turnover is concerned, this possibility is assumed to be catalytically negligible for kinetic reasons (slow release). (4) There is ample evidence for slow interconversion of substrates in the T state (unisite catalysis). But a T state with tightly bound ADP and P_i that now rapidly forms bound ATP does not appear likely to be an intermediate in the catalysis [7,42] (for a more explicit view see also [43]). Therefore, Boyer suggested that substrate interconversion in the T state probably does not occur during rapid phosphorylation. Taking up this suggestion, our modeling concept associates substrate conversion with the L↔T transition. Conversion in the T state is regarded as a side reaction. Taking together, statements (1)–(4) prove rapid turnover to depend on the realization of a trisite catalysis mechanism where all three binding sites are permanently occupied by nucleotides. In detail, during synthesis sites O/L/T are occupied by ATP/ADP/ATP and during hydrolysis by ADP/ADP/ATP. The binding change concept presented here resembles that of Senior et al. [44] which was based on a completely different experimental approach, namely measurement of site occupancy by a tryptophan fluorescence label.

The above described binding change concept may be discussed further with respect to its suitability for the interpretation of substrate-velocity relationships in the range from unisite to multisite conditions. Hydrolysis measurements yielded two K_m values of roughly 15 nM ($v_{max} \approx 0.1$ s^{-1}) and 150 μM ($v_{max} \approx 200$ s^{-1}) [36,45]. The low K_m value has been attributed to slow unisite catalysis where only the T site is involved in ATP binding, nucleotide conversions and ADP release [40]. The absence of a binding change is supported by the fact that unisite catalysis is not linked to rotation of subunit γ [46]. The high K_m value provoking rapid turnover is attributable to trisite catalysis according to the binding change concept of Fig. 2. In this case ATP binding to the O site is followed by the binding change sequence O→T→L→O and release of ADP from the newly formed O site. Alternatively, Boyer et al. [43,45] prefer a bisite mechanism, where release of ADP occurs already from the L site (further discussion of this discrepancy later on). Investigation of ATP synthesis also yields two K_m values of roughly 1 μM ($v_{max} \approx 5$ s^{-1}) and 30 μM ($v_{max} \approx 200$ s^{-1}) [35,47]. The low value again has been attributed to slow unisite catalysis [39]. In this case the T site is involved in ADP binding and nucleotide conversion and ATP release occurs from the O site which has to be formed from the ATP loaded T site by a H^+-driven binding change. Likewise a bisite mechanism might be postulated where ADP binding to the L site is followed by a slow H^+-driven binding change sequence

L→T→O and ATP release from the O site. However, this interpretation of the low K_m value is in conflict with results of Zhou and Boyer [42] who measured in the presence of 2 μM ADP only one bound nucleotide per synthase. The high value again is attributable to rapid trisite catalysis according to the binding change concept of Fig. 2. In this case ADP binding to the O site is followed by a H^+-driven binding change sequence O→L→T→O and ATP release from the newly formed O state. Again, this interpretation is questioned by Boyer's concept of a bisite mechanism where ADP, in contrast to ATP, binds preferentially to the L site [42,43]. However, such an interpretation does not correspond to the evidence of competitive binding of ADP and ATP mentioned above [21,41]. Evidently more experimental work is needed to answer the question of site occupancy unequivocally.

5.5. Substrate specificity

The rate constants for binding of ATP, ADP, P_i in Table 1, specified as k_{ATP}, k_{ADP}, k_P, are related to the total amount of substrate species in each case. Evidence has now been accumulated that the real binding species are the magnesium ion nucleotide complexes $MgATP^{2-}$, $MgADP^-$ [48] and the twofold protonated phosphate species $H_2PO_4^-$ [49]. The corresponding binding rate constants may be calculated according to the relation $k_{\text{ion complex}} = k_{\text{total amount}}/x_{\text{ion complex}}$, where x denotes the mole fraction of the ion complex. The x values may be calculated with recourse to a procedure of Krab and van Wezel [50] taking into account the complex ions H^+, Mg^{2+} and K^+ [41]. The experimental conditions used here (pH = 8.00, pMg = 2.52, pK = 1.30, T = 293 K, I = 0.07 M) yield numbers of $x_{MgATP^{2-}} = 0.97$, $x_{MgADP^-} = 0.72$, $x_{H_2PO_4^-} = 0.05$. On this basis we transform the rate constants for substrate binding of Table 1 to ion complex-related values of $x_{MgATP^{2-}} = 2.14 \cdot 10^6$ M^{-1} s^{-1}, $x_{MgADP^-} = 1.24 \cdot 10^7$ M^{-1} s^{-1}, $x_{H_2PO_4^-} = 1.58 \cdot 10^7$ M^{-1} s^{-1}. In contradiction to the total amount-related values of Table 1, these values are independent of the experimental conditions (except genuine influence of temperature and ionic strength).

5.6. Side path routes

In this paper we described the catalytic pathways of the CF_0F_1-ATP synthase. No attention has been paid to possible side path reaction routes. Examples are the proton slip reaction in the absence of nucleotides [34] and the inactivation reaction where ADP is occluded in the T state instead of ATP [51]. These extra routes will be treated in a forthcoming paper (O. Pänke, B. Rumberg, in preparation).

Acknowledgements

The authors would like to thank Drs. D.A. Cherepanov and A.Y. Mulkidjanian from the Division of Biophysics of the University of Osnabrück for drawing their attention to [30].

Appendix

A.1. Derivation of Eq. 9

The onset equation

$$\frac{A_j}{A_0} = \frac{A_1}{A_2}\cdot\frac{A_2}{A_3} \cdots \frac{A_j}{A_{j-1}}$$

transforms after insertion of Eqs. 3 and 8 to

$$A_j = A_0 \cdot \exp\left[-\left(\Delta\tilde{\mu}_{H^+}\cdot j + \alpha\cdot\sum_{x=1}^{j}(2x-1)/RT\right]\right.$$

which finally changes to

$$A_j = A_0 \cdot \exp\left[-\left(\Delta\tilde{\mu}_{H^+}\cdot j + \alpha\cdot j^2\right)/RT\right]$$

A.2. Proof of the Gaussian character of Eq. 9

The core function of Eq. 9

$$\exp\left[-\left(\Delta\tilde{\mu}_{H^+}\cdot j + \alpha\cdot j^2\right)/RT\right]$$

may be rearranged to

$$\exp\left[\frac{\Delta\tilde{\mu}_{H^+}^2}{4\alpha\cdot RT}\right]\cdot\exp\left[-\frac{\alpha}{RT}\cdot\left(j + \frac{\Delta\tilde{\mu}_{H^+}}{2\alpha}\right)^2\right]$$

where the second exponential unveils the Gaussian character of the onset function.

A.3. Proof of the equivalence of Eqs. 9 and 16

The core function of Eq. 16

$$\exp[-(\Delta\tilde{\mu}_{H^+}\cdot j + \alpha\cdot j^2)/RT]\cdot\exp[8\alpha\cdot\kappa\cdot(j-2\kappa)/RT]$$

may be rearranged to

$$\exp\left[-\frac{4\kappa\cdot\Delta\tilde{\mu}_{H^+}}{RT}\right]\cdot\exp\left[\frac{\Delta\tilde{\mu}^2_{H^+}}{4\alpha\cdot RT}\right]\cdot$$

$$\exp\left[-\frac{\alpha}{RT}\cdot\left((j-4\kappa)+\frac{\Delta\tilde{\mu}_{H^+}}{2\alpha}\right)^2\right]$$

which corresponds to the phase-shifted function of Appendix A.2.

References

[1] P.D. Boyer, Annu. Rev. Biochem. 66 (1997) 717–749.
[2] H.S. Walraven, H. Strotmann, O. Schwarz, B. Rumberg, FEBS Lett. 379 (1996) 309–313.
[3] S. Berry, B. Rumberg, Biochim. Biophys. Acta 1276 (1996) 51–56.
[4] O. Pänke, B. Rumberg, Biochim. Biophys. Acta 1322 (1997) 183–194.
[5] R.L. Cross, L. Taiz, FEBS Lett. 259 (1990) 227–229.
[6] P.D. Boyer, W.E. Kohlbrenner, in: B.R. Selman, S. Selman-Reimer (Eds.), Energy Coupling in Photosynthesis, Elsevier/North-Holland, Amsterdam, 1981, pp. 231–240.
[7] P.D. Boyer, Biochim. Biophys. Acta 1140 (1993) 215–250.
[8] J.P. Abrahams, A.G.W. Leslie, R. Lutter, J.E. Walker, Nature 370 (1994) 621–628.
[9] J. Weber, S. Wilke-Mounts, R.S.F. Lee, E. Grell, A.E. Senior, J. Biol. Chem. 268 (1993) 20126–20133.
[10] T.M. Duncan, V.V. Bulygin, Y. Zhou, M.L. Hutchinson, R.L. Cross, Proc. Natl. Acad. Sci. USA 92 (1995) 10964–10968.
[11] D. Sabbert, S. Engelbrecht, W. Junge, Nature 381 (1996) 623–626.
[12] H. Noji, R. Yasuda, M. Yoshida, K. Kinosita, Nature 386 (1997) 299–302.
[13] R. Aggeler, I. Ogilvie, R.A. Capaldi, J. Biol. Chem. 272 (1997) 19621–19624.
[14] D. Sabbert, W. Junge, Proc. Natl. Acad. Sci. USA 94 (1997) 2312–2317.
[15] K. Häsler, S. Engelbrecht, W. Junge, FEBS Lett. 426 (1998) 301–304.
[16] R. Yasuda, H. Noji, K. Kinosita, M. Yoshida, Cell 93 (1998) 1117–1124.
[17] W. Junge, H. Lill, S. Engelbrecht, Trends Biochem. Sci. 22 (1997) 420–423.
[18] S.B. Vik, B.J. Antonio, J. Biol. Chem. 269 (1994) 30364–30369.
[19] T. Elston, H. Wang, G. Oster, Nature 391 (1998) 510–513.
[20] S. Engelbrecht, W. Junge, FEBS Lett. 414 (1997) 485–491.
[21] O. Pänke, B. Rumberg, FEBS Lett. 383 (1996) 196–200.
[22] O. Pänke, B. Rumberg, in: G. Garab (ed), Photosynthesis: Mechanism and effects, Vol III, Kluwer Academic Publishers, Dordrecht, 1998, 1643–1648.
[23] P. Turina, Bioelectrochem. Bioenerg. 33 (1994) 31–43.
[24] U. Junesch, P. Gräber, FEBS Lett. 294 (1991) 275–278.
[25] H.L. Huber, B. Rumberg, U. Siggel, Ber. Bunsenges. Phys. Chem. 84 (1980) 1050–1055.
[26] R. Tiemann, H.T. Witt, Biochim. Biophys. Acta 681 (1982) 202–211.
[27] R.H. Fillingame, Curr. Opin. Struct. Biol. 6 (1996) 491–498.
[28] M.M. Hingorani, M.T. Washington, K.C. Moore, S.S. Patel, Proc. Natl. Acad. Sci. USA 94 (1997) 5012–5017.
[29] B.L. Stitt, Y. Xu, J. Biol. Chem. 273 (1998) 26477–26486.
[30] Y. Tsuda, H. Yasutake, A. Ishijima, T. Yanagida, Proc. Natl. Acad. Sci. USA 93 (1996) 12937–12942.
[31] Gerthsen, Physik, Springer-Verlag, Berlin, 1997, p. 131.
[32] F.E. Possmeyer, P. Gräber, J. Biol. Chem. 269 (1994) 1896–1904.
[33] G. Kaim, P. Dimroth, FEBS Lett. 434 (1998) 57–60.
[34] G. Groth, W. Junge, Biochemistry 32 (1993) 8103–8111.
[35] A. Labahn, P. Gräber, Biochim. Biophys. Acta 1144 (1993) 170–176.
[36] A. Labahn, P. Gräber, Biochim. Biophys. Acta 1141 (1993) 288–296.
[37] M.K. Al-Shawi, A.E. Senior, Biochemistry 31 (1992) 878–885.
[38] C. Grubmeyer, R.L. Cross, H.S. Penefsky, J. Biol. Chem. 257 (1982) 12092–12100.
[39] A. Labahn, P. Fromme, P. Gräber, FEBS Lett. 271 (1990) 116–118.
[40] P. Gräber, A. Labahn, Bioenerg. Biomembr. 24 (1992) 493–497.
[41] O. Pänke, Thesis, Wissenschaft und Technik Verlag, Berlin, 1997.
[42] J.M. Zhou, P.D. Boyer, J. Biol. Chem. 268 (1993) 1531–1538.
[43] P.D. Boyer, Biochim. Biophys. Acta 1365 (1998) 3–9.
[44] J. Weber, C. Bowman, A.E. Senior, J. Biol. Chem. 271 (1996) 18711–18718.
[45] Y. Milgrom, M.B. Murataliev, P.D. Boyer, Biochem. J. 330 (1998) 1037–1043.
[46] J.J. Garcia, R.A. Capaldi, J. Biol. Chem. 273 (1998) 15940–15945.
[47] S.D. Stroop, P.D. Boyer, Biochemistry 24 (1985) 2304–2310.
[48] A.E. Senior, R.S.F. Lee, M.K. Al-Shawi, J. Weber, Arch. Biochem. Biophys. 297 (1992) 340–344.
[49] S. Fischer, Thesis, Freiburg, 1998.
[50] K. Krab, J. van Wezel, Biochim. Biophys. Acta 1098 (1992) 172–176.
[51] D. Lohse, H. Strotmann, Biochim. Biophys. Acta 976 (1989) 94–101.